Solar and Stellar Multi-scale Activity
Proceedings IAU Symposium No. 400, 2026
S. Vargas-Domínguez & J. C. Buitrago-Casas, eds.
doi:10.1017/S174392132610684X

Solar photospheric spectrum microvariability

Dainis Dravins[1] and Hans-Günter Ludwig[2]

[1]Lund Observatory, Division of Astrophysics, Department of Physics, Lund University, SE-22100 Lund, Sweden
email: dainis@astro.lu.se

[2]Zentrum für Astronomie der Universität Heidelberg, Landessternwarte, Königstuhl 12, DE–69117 Heidelberg, Germany

Abstract. Finding low-mass planets around solar-type stars requires understanding the physical variability of the host star, which greatly exceeds the planet-induced radial-velocity modulation. This project aims to analyze – observationally and theoretically – the character and physical origins of fluctuations in solar photospheric absorption lines.

Observationally, photospheric equivalent-width variations were measured in 1000 selected spectra from three years of HARPS-N data of the Sun-as-a-star, showing changes that largely shadow the chromospheric Ca II H&K activity-cycle signal, but with much smaller amplitudes on sub-percent levels. Among iron lines, the greatest are for Fe II in the blue, while the trends change sign among lines in the green Mg I triplet and between Balmer lines. No variation was seen in the semi-forbidden Mg I 457.1 nm.

Theoretically, hydrodynamic 3D modeling of solar surface convection produces time sequences of synthetic high-resolution spectral atlases. Radial velocities averaged over small simulation areas jitter by some ± 150 m s^{-1}, scaling to $\sim\pm 2$ m s^{-1} for the full solar disk on timescales of granular convection. Among different lines, jittering is in phase, but the amplitudes differ by about one tenth of their values: greater for stronger and ionized lines, decreasing at longer wavelengths

Keywords. Sun: spectrum, Sun: photosphere, Exoplanets: radial velocities, Exoplanets: terrestrial planets

1. Introduction

Efforts are underway to enable the detection of 'exoEarths', i.e., planets of about one Earth mass, in approximately one-year orbits around solar-type stars. The most promising method appears to be the radial-velocity one, with instrumental precisions now approaching 10 cm s^{-1} (Crass et al. 2021; Fischer et al. 2016; Rackham et al. 2023). However, such an exoplanet signal is overwhelmed by intrinsic stellar variability, where the currently best modeling is unable to extract planetary signals with amplitudes much below 1 or 2 m s^{-1}. To reach adequate sensitivity, it is essential to understand the complexities of stellar atmospheric dynamics and spectral line formation, which manifest as a physical jitter or drift of its apparent radial velocity. A step toward exoEarth detection could be to identify dissimilar spectral lines (e.g., strong or weak, neutral or ionized, high or low excitation, atomic or molecular, short or long wavelength, magnetically sensitive or not), with disparate responses to stellar activity, which are modulated in a characteristic manner, to disentangle wavelength shifts induced by exoplanets from those originating in solar-type atmospheres.

As measures of stellar activity, chromospheric indices are often used, in particular, Ca II H&K. However, precision radial velocities are measured in photospheric lines only,

© The Author(s), 2026. Published by Cambridge University Press on behalf of The International Astronomical Union. This is an Open Access article, distributed under the terms of the Creative Commons Attribution licence (https://creativecommons.org/licenses/by/4.0/), which permits unrestricted re-use, distribution and reproduction, provided the original article is properly cited.

https://doi.org/10.1017/S174392132610684X Published online by Cambridge University Press

for which chromospheric indices can, at best, be only an approximation. For example, while fluctuations in apparent solar photospheric radial velocities overall correlate with Ca II H&K indices, there is a time lag of several days between them, seemingly due to the photospheric signal being more dependent on the areal extent of magnetic plage regions than on the centres of chromospheric emission (Bruning & Labonte 1985; Collier Cameron et al. 2019), requiring studies of microvariability in specifically photospheric absorption lines.

This project studies the properties and origins of fluctuations in different classes of absorption lines in solar-type spectra. To develop optimal algorithms for the extraction of radial velocities from observational data, a detailed understanding of how stellar physical variability affects different photospheric lines will most likely be required. Besides leading to improved data extraction from current instruments, such an understanding should also provide guidance regarding the types of future instrumentation that may be required for exoEarth surveys.

2. Line-strength variability during the solar cycle

Past efforts to identify solar-cycle variability of photospheric lines in the spectrum of the Sun-as-a-star included 35 years of monitoring from Kitt Peak (Livingston et al. 2007, 2010), but the results were rather inconclusive, except for chromospherically influenced lines. This acknowledges the challenges in maintaining stable instrumentation and observational conditions over longer epochs with spectrometers operated in air and readjusted between different observing programs. A review of these and other earlier efforts is in Dravins & Ludwig (2024).

These limitations are now circumvented by Sun-as-a-star telescopes feeding extreme-precision radial-velocity spectrometers operated in a vacuum and (almost) without any readjustments. Their time series permits not only radial-velocity monitoring but also precise stellar spectroscopy.

2.1. *HARPS-N observations of the Sun-as-a-star*

On La Palma, a small sunlight-integrating telescope feeding the HARPS-N spectrometer continues to observe the Sun-as-a-star. Its first public data release covered the three-year period from July 2015 through July 2018, a declining phase of the solar activity cycle (Collier Cameron et al. 2019; Dumusque et al. 2021; Milbourne et al. 2019). Those spectra, with a spectral resolution $\lambda/\Delta\lambda \sim$115,000, cover the wavelength interval of 387-691 nm.

Out of approximately 35,000 recordings in that dataset, 1000 spectra were selected for the best photometric signal-to-noise (typically ∼350) and the smallest airmass (minimizing effects from telluric absorption), singling out summertime observations around daily noon (for the La Palma latitude, which is then close to zenith) during 2016, 2017, and 2018. Groups of largely unblended lines were chosen: Fe I of varying strengths between 430–685 nm; Fe II lines in the blue, stronger lines such as the green Mg I triplet, the semi-forbidden intercombination line Mg I 457.1 nm, the molecular G-band, hyperfine split Mn I lines, and also the chromospherically influenced Balmer lines, Na I D_1 and D_2. For details, see Dravins & Ludwig (2024).

2.2. *Photospheric line changes during successive years*

Figure 1 shows systematic patterns in measured line-strength variations. With increasing chromospheric activity, Fe absorption gradually weakens, showing the greatest

https://doi.org/10.1017/S174392132610684X Published online by Cambridge University Press

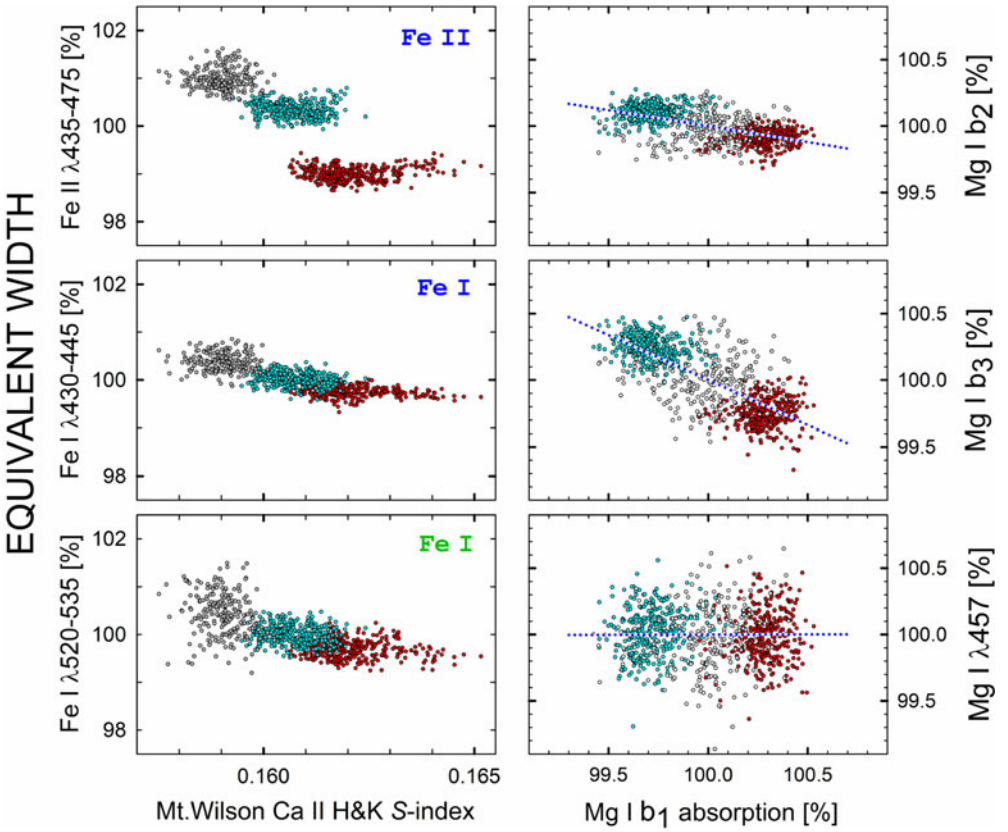


Figure 1. Left: Observed relative changes of Fe I and Fe II absorption line equivalent widths in the spectrum of the Sun-as-a-star, measured with HARPS-N, between summer seasons in 2016 (red), 2017 (cyan), and 2018 (gray), as a function of the Mt.Wilson Ca II H&K chromospheric activity S-index. The variability largely shadows the Ca II H&K activity-cycle signal, but with much smaller amplitudes on sub-percent levels. Right: Relative and systematic changes in the absorption equivalent widths between the three strong lines of the Mg I green triplet, and the semiforbidden Mg I λ457 nm line.

amplitude for Fe II at shorter wavelengths, while diminishing for Fe I and at longer wavelengths.

For stronger, chromospherically influenced lines such as the green triplet of Mg I b_1 518.3, b_2 517.2, and b_3 516.7 nm, the behavior is more complex, and the changes are systematically different among the lines in this triplet. Their atomic energy levels are coupled by transitions between a common upper level and three different lower levels, a configuration that makes non-LTE effects very likely. Somewhat similar relations are observed among the Hα, Hβ, and Hγ Balmer lines of hydrogen. By contrast, the formation of the semi-forbidden Mg I 457.1 nm intercombination line is expected to be relatively simple, being dominated by atomic collisions. Indeed, its behavior is very different, showing no significant variability during these years.

Such patterns of photospheric line variability demonstrate that they contain nontrivial information and measure something different from chromospheric indices. However, detailed studies of such signals at their sub-percent levels remain challenging. With equivalent-width measures formed over many tens of pixels in the spectrometer, each with a nominal S/N ~350, and after averaging over several similar lines, one would

https://doi.org/10.1017/S174392132610684X Published online by Cambridge University Press

expect the photometric noise contribution to be less than 0.001, raising the question of what part of the scatter seen in Fig. 1 is physical and what is instrumental?

It would certainly be interesting to follow the relative radial-velocity and line-shape changes between groups of different classes of lines during the solar activity cycle; however, that remains beyond the capabilities of current radial-velocity instruments. Their wavelength calibration is stable but not absolute between different grating orders. They reach sub-m s^{-1} precision, but only after averaging over complete stellar spectra, not for limited groups of selected lines. Although their spectral resolutions are classed as 'high', those are lower than in synthetic spectra or in spectrometers at solar telescopes, smearing out signatures such as the exact bisector shapes. For HARPS-N and similar instruments, such limitations are discussed by Hanassi-Savari et al. (2025). For such reasons, the current studies concern equivalent widths only, which – at least to a first approximation – should be insensitive to such issues.

Several precision radial-velocity instruments are used to monitor the Sun-as-a-star, and comparisons among them confirm that their deduced radial-velocity fluctuations largely agree Zhao et al. (2023). With time series now reaching a full solar cycle, it should be feasible to examine whether the deduced line-strength variations also agree among the instruments, thereby isolating what is solar and what is instrumental.

3. Theoretical modeling of radial-velocity jittering

Quiet granulation covers most of the solar surface and provides most of the solar flux. For its modeling, surface convection is simulated with time-dependent 3D hydrodynamics, along with the concurrent computation of complete spectra from ultraviolet to infrared. With hyper-high spectral resolution, the changing shapes and wavelength shifts of representative Fe I and Fe II lines are followed during the simulation sequences, seeking systematic patterns of variability, particularly those that correlate with excursions in apparent radial velocity.

Solar surface volumes that realistically can be simulated cover only a small surface fraction: in the present modeling with the CO^{5}BOLD code this is a 3D Cartesian "local-box" model of 5.6×5.6 Mm^2; for modeling methodology, see Freytag et al. (2012). From this simulation volume, spatially averaged line profiles are computed in LTE at various emergent angles, and corresponding full-disk profiles synthesized for a non-rotating Sun. The radial-velocity jittering for integrated sunlight, built up from such a small simulation area, typically amounts to ± 150 m s^{-1}, scaling to $\sim$2 m s^{-1} for the real full solar disk. Most photospheric lines vary in phase but differences in radial-velocity excursions between various line-groups are found to be about 10% of their values. Amplitudes are greater for stronger and for ionized lines, decreasing at longer wavelengths. An example is in Fig. 2 with details in Dravins & Ludwig (2023).

Current computational constraints do not permit properly conducting detailed simulations of granulation coupled with large-scale features such as supergranular and meridional flows, p-mode oscillations, and others, which certainly may contribute significant radial-velocity signals but would require much larger simulation volumes.

3.1. *Possible mechanism of differences between line-groups*

For solar-type stars, the greatest convective blueshifts are found in weak lines formed in the deeper photosphere. However, the variability is found to be smallest in these weak lines, increasing for stronger lines formed in the upper photosphere. A typical 3D atmospheric structure, e.g., Fig. 14 in Nordlund et al. (2009) shows the smallest temperature fluctuations to occur at optical depths around $\tau = 0.3$, reaching greater values both deeper down and higher up. Weaker spectral lines form around $\tau = 0.5$, where

https://doi.org/10.1017/S174392132610684X Published online by Cambridge University Press

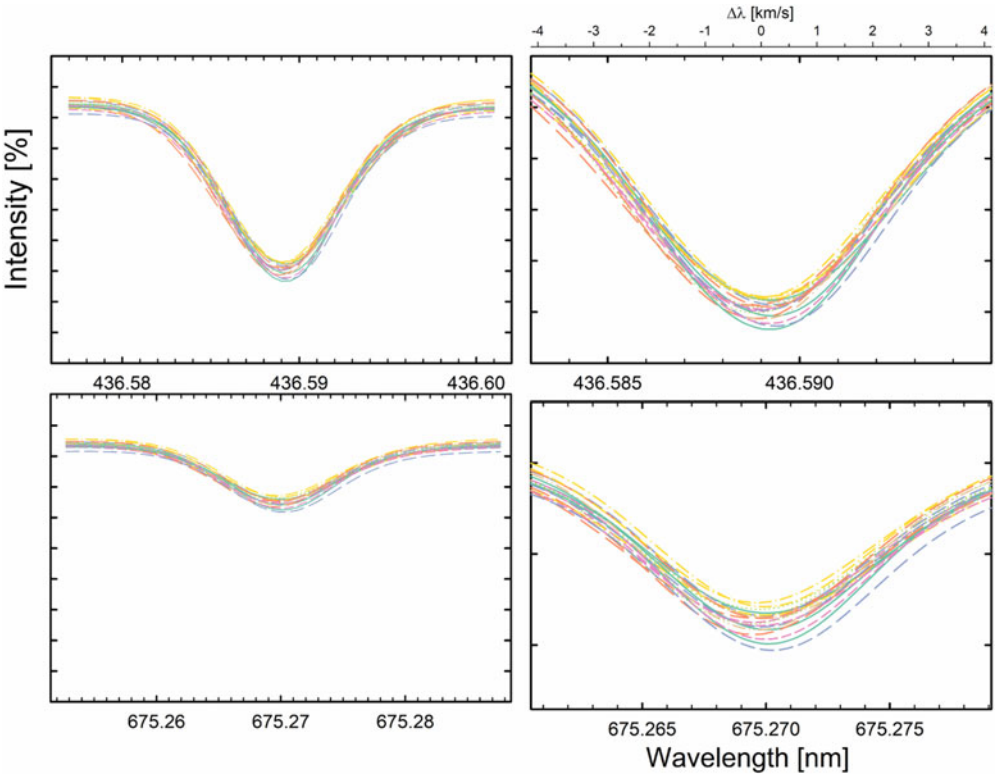


Figure 2. Synthetic spectral lines for the spectrum of a full solar disk, built up by spectral-line components from a small simulation area of non-magnetic granulation, sampled at 20 instances during the 3D hydrodynamic simulation. Top: A strong Fe I line in the blue, λ436.59 nm, $\chi = 2.99$ eV. Bottom: A weak Fe I line in the longward red, λ675.27 nm, $\chi = 4.64$ eV. Right: zoomed-up line centers on a uniform wavelength scale in units of radial velocity (top); tick marks on the vertical axes correspond to those for the full profiles. Hyper-high spectral resolution, $\lambda/\Delta\lambda$ ~900,000.

the fluctuations are smaller than those at the higher formation heights of the stronger lines with lower atmospheric densities, where the gasses may roam more freely and the lines may experience greater jittering amplitudes.

3.2. *Testing model predictions?*

Due to their small size, some model predictions are not easily verified in current observations of the Sun-as-a-star. However, the modeling may be tested with spatially resolved observations across the solar disk. The radial-velocity jittering is predicted to be greatest at the disk center, gradually decreasing toward the limb, with different behavior for stronger and weaker lines and for those of different excitation potentials (Dravins & Ludwig 2023). While the disk-integrated signal amplitudes differ by only a fraction of a $\mathrm{m\,s^{-1}}$, the signal over an area of a few arcminutes is greater by orders of magnitude and should be realistic to sample.

4. Magnetic granulation

The second largest contribution to solar irradiance comes from the plage and faculae areas of magnetic granulation. Magnetic fields disturb and dampen the convective velocity patterns, causing different asymmetries in the line profiles and resulting in much smaller

https://doi.org/10.1017/S174392132610684X Published online by Cambridge University Press

convective blueshifts. The varying area coverage of magnetic granulation during the solar cycle has been identified as the main driver of long-term changes in solar apparent radial velocity (Meunier et al. 2010a,b). While contributions from sunspots also affect spectral lines (Komori et al. 2025), their fraction of the solar photospheric flux is modest.

While non-magnetic granulation in full-disk spectra, in principle, can be modeled from fundamental physical parameters of stellar temperature, gravity, and chemical composition, there are more degrees of freedom for magnetic granulation. Not only can their area coverage and latitudinal and longitudinal surface distributions be different (and unknown for other stars), but also the degree and distribution of magnetic flux concentrations. For the spectral synthesis, an additional complication (or opportunity!) arises with the potential of handling the components of magnetically sensitive lines in a situation characterized by a sometimes uneven precision of laboratory data.

Nevertheless, line-profile variability in magnetic areas could reveal signatures that might discriminate against other effects. A sequence of magnetohydrodynamic CO^{5}BOLD solar models was computed as above, representing a range of magnetic flux densities. The vertical magnetic flux through the atmosphere was fixed by initial conditions and preserved during the modeling sequence. Field lines were constrained to pass vertically through the top and bottom boundaries of the simulation volume. For details, including synthetic surface images for different magnetic flux levels and at different limb angles, see Ludwig et al. (2023). Synthetic LTE spectra for different flux densities were computed at numerous instances throughout the simulations, and Fig. 3 provides some examples for 2400 G (240 mT), compared to the non-magnetic case.

5. Outlook: possibilities and challenges

A significant addition to Sun-as-a-star facilities will be the PoET telescope, to be installed at ESO VLT on Paranal (Santos et al. 2025). Besides providing spectra of the Sun-as-a-star with the ESPRESSO spectrometer's higher resolving power of ∼200,000, it will be able to select limited portions of the solar disk to examine local radial velocities. This should help to identify locations contributing to solar velocity jittering and also enable novel tests of hydrodynamic model atmospheres. Until now, these have been verified against spatially and temporally averaged spectral line shapes, granulation morphology, and intensity modulation. Predictions such as different radial velocity jittering amplitudes among various classes of spectral lines – such as discussed above – cannot yet be tested because of lack of adequate instrumentation. For Sun-as-a-star, it is still not possible to discern differences between line-group jittering of amplitudes between, say, 2.0 and 2.2 $\mathrm{m\,s^{-1}}$, as deduced for the full solar disk. However, such extrapolated full-disk values emanate from small simulation areas where the amplitudes are much greater and should be readily measurable with ESPRESSO.

Different levels of approximation and sophistication are possible in computing synthetic spectral lines from dynamic 3-D atmospheres, eventually envisioning 'full' non-LTE treatments with Zeeman-sensitive line components, a connection to the lower chromosphere, and others. Although not all such observations are yet feasible, the types of observations foreseen with PoET may well guide us toward highly precise 3-D spectra. To realize corresponding spatially resolved spectroscopy across the surfaces of other stars is marginally possible using exoplanet transits to differentially isolate surface portions, for which theoretical line-profile predictions can be made (Dravins et al. 2017a,b, 2018, 2021a,b). In the nearish future, the availability of stable spectrometers at extremely large telescopes should make such observations less challenging.

The significance of non-LTE effects for also 'ordinary' photospheric lines measured for radial velocities is suggested by studies of how different assumed levels of chromospherically influenced temperatures in the upper photosphere affect 1-D non-LTE line

https://doi.org/10.1017/S174392132610684X Published online by Cambridge University Press

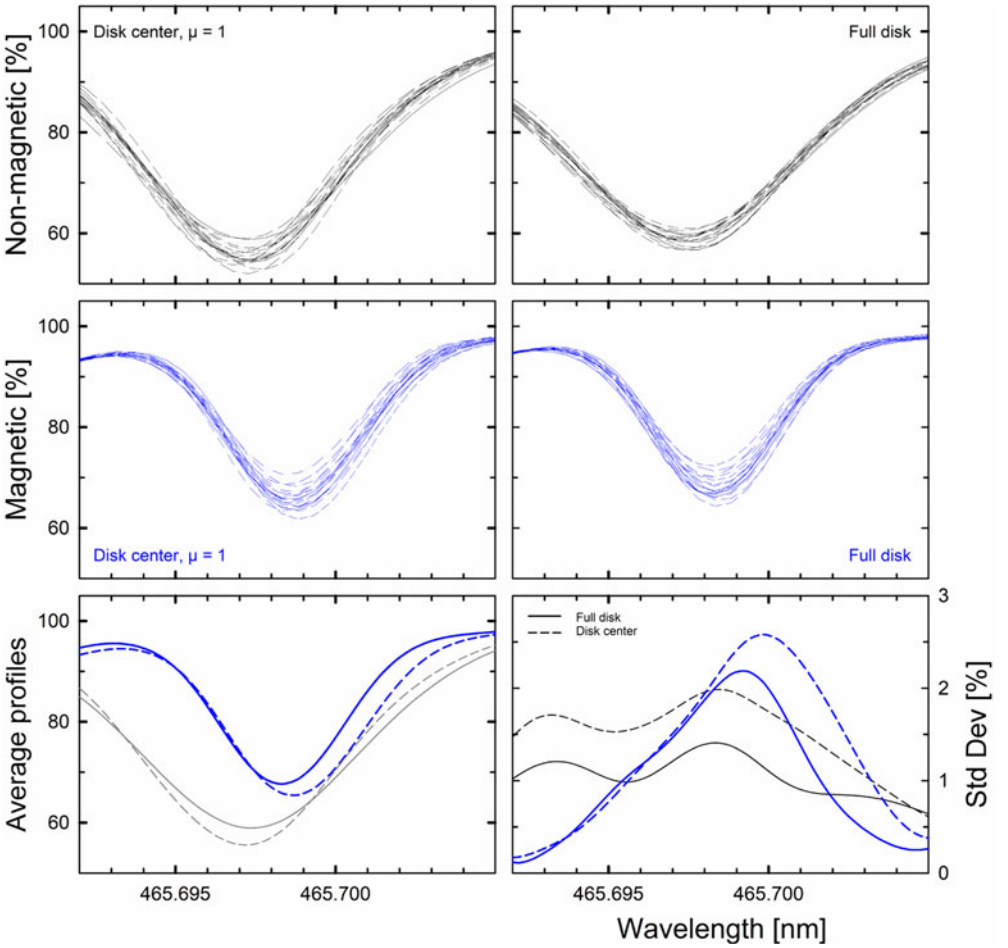


Figure 3. Synthetic solar profiles for an ordinary Fe II line ($\lambda = 465.698$ nm, $\chi = 2.89$ eV) in non-magnetic and magnetic (2400 G, 240 mT) granulation. Thin curves are spatially averaged profiles across the simulation area, sampled at 20 temporal instances; black for non-magnetic; blue for magnetic. Left-hand groups show profiles at solar disk center, at right integrated for a full (non-rotating) solar disk, using center-to-limb profiles from the small simulation area. Spatially and temporally averaged profiles are at bottom left. The non-magnetic convective blueshift is greater (by ~ 400 m s^{-1}), and furthermore is slightly larger at disk center than in integrated sunlight. The opposite holds for magnetic granulation, apparently caused by a more 'corrugated' stellar surface, an effect also causing increased plage and faculae brightness toward the limb (Ludwig et al. 2023). Bottom right: Hyper-high spectral resolution ($\lambda/\Delta\lambda$ ~900,000) enables to study variations inside line profiles. The temporal standard deviations show the longward line flanks to be the most variable in magnetic granulation versus the line core in the non-magnetic case.

formation in modeled G2 V stars (Vieytes et al. 2025). The response to different levels of chromospheric heating is markedly different among various Fe I lines, even those with similar strengths at nearby wavelengths, carrying a promise that they may contain additional and perhaps unique signatures of solar atmospheric modulation. Such lines could be selected to observationally search for their variability, although challenging non-LTE 3D calculations might be needed for a fuller understanding.

Other relevant spectrometers for Sun-as-a-star spectroscopy include those in the near infrared, e.g., NIRPS at ESO on La Silla (Bouchy et al. 2025). As seen in both observed

https://doi.org/10.1017/S174392132610684X Published online by Cambridge University Press

and synthetic spectra, the amplitudes of physical variability decrease toward longer wavelengths, suggesting that the near infrared could be advantageous for exoEarth searches. However, there is the complexity of fewer atomic lines of significant strength in that region, as well as effects from enhanced telluric absorption.

The large ANDES spectrometer is being built for the ESO ELT (Palle et al. 2025). While it will, of course, have outstanding light-collecting power and should provide very high S/N spectra for brighter stars, the challenges of interfacing a realistically large cross-dispersed échelle spectrometer to an extremely large telescope limit its spectral resolution to ranges similar to those of current instruments. In the longer term, one could certainly wish for hyper-high resolutions of 1,000,000, which may possibly require diffraction-limited adaptive-optics photonic instruments to limit their physical size. Already, NIRPS is taking advantage of adaptive optics to limit its size, but realizing the same for an extremely large telescope in the shorter visual wavelengths remains an interesting challenge.

Acknowledgements. The work by DD is supported by grants from The Royal Physiographic Society of Lund. Extensive use was made of NASA's ADS Bibliographic Services and the arXiv distribution service.

References

Bouchy, F., Doyon, R., Pepe, F., et al. 2025, *A&A*, 700, A10
Bruning, D. H. & Labonte, B. 1985, *Solar Phys.*, 97, 1
Collier Cameron, A., Mortier, A., Phillips, D., et al. 2019, *MNRAS*, 487, 1082
Crass, J., Gaudi, B. S., Leifer, S., et al. 2021, arXiv:2107.14291
Dravins, D., Ludwig, H.-G., Dahlén, E., et al. 2017a, *A&A*, 605, A90
Dravins, D., Ludwig, H.-G., Dahlén, E., et al. 2017b, *A&A*, 605, A91
Dravins, D., Gustavsson, M., & Ludwig, H.-G. 2018, *A&A*, 616, A144
Dravins, D., Ludwig, H.-G., & Freytag, B. 2021a, *A&A*, 649, A16
Dravins, D., Ludwig, H.-G., & Freytag, B. 2021b, *A&A*, 649, A17
Dravins, D., Ludwig, H.-G. 2023, *A&A*,679, A3
Dravins, D., Ludwig, H.-G. 2024, *A&A*, 687, A60
Dumusque, X., Cretignier, M., Sosnowska, D., et al. 2021, *A&A*, 648, A103
Fischer, D. A., Anglada-Escude, G., Arriagada, P., et al. 2016, *PASP*, 128, 066001
Freytag, B., Steffen, M., Ludwig, H.-G., et al. 2012, J. Comp. Phys., 231, 919
Hanassi-Savari, F., Pietrow, A. G. M., Druett, M. K., et al. 2025, arXiv:2508.07912
Komori, C., Brewer, J. M., & Zhao, L. L. 2025, arXiv:2508.09030
Livingston, W., Wallace, L., White, O. R., et al. 2007, *ApJ*, 657, 1137
Livingston, W., White, O. R., Wallace, L., et al. 2010, *MemSAIt*, 81, 643
Ludwig, H.-G., Steffen, M., & Freytag, B. 2023, *A&A*, 679, A65
Meunier, N., Desort, M., & Lagrange, A.-M. 2010a, *A&A*, 512, A39
Meunier, N., Lagrange, A.-M., & Desort, M. 2010b, *A&A*, 519, A66
Milbourne, T. W., Haywood, R. D., Phillips, D. F., et al. 2019, *ApJ*, 874, 107
Nordlund, Å., Stein, R. F., & Asplund, M. 2009, Living Rev. Solar Phys., 6, 2
Palle, E., Biazzo, K., Bolmont, E., et al. 2025, Exp. Astron., 59, 29
Rackham, B. V., Espinoza, N., Berdyugina, S. V., et al. 2023, RAS Techn. Instrum., 2, 148
Santos, N. C., Cabral, A., Leite, I., et al. 2025, The Messenger, 194, 21
Vieytes, M. C., Zhao, L. L., & Bedell, M. 2025, *ApJ*, 981, 4
Zhao, L. L., Dumusque, X., Ford, E. B., et al. 2023, *AJ*, 166, 173

https://doi.org/10.1017/S174392132610684X Published online by Cambridge University Press